

Anomalous nuclear-spin heat capacities in submonolayer solid ^3He adsorbed on graphite

M. Morishita and H. Nagatani

Institute of Physics, University of Tsukuba, Tsukuba, Ibaraki 305-8571, Japan

Hiroschi Fukuyama

Department of Physics, Graduate School of Science, University of Tokyo, 7-3-1 Hongo, Bunkyo-ku, Tokyo 113-0033, Japan

(Received 26 April 2001; published 4 March 2002)

Nuclear-spin heat capacities of submonolayer solid ^3He adsorbed on a graphite surface are measured down to 100 μK , a factor of 20 lower temperature than in previous works. This system is one of the most ideal two-dimensional quantum spin systems ($S=1/2$). In a wide areal density region ($6.1\text{ nm}^{-2}\leq\rho\leq 8.7\text{ nm}^{-2}$), anomalous temperature dependencies of the heat capacity, $C\propto T^\alpha$ ($-1.6\leq\alpha\leq-0.7$), are observed in a temperature range over two orders of magnitude ($0.1\text{ mK}\leq T\leq 20\text{ mK}$) instead of the expected high-temperature behavior ($\alpha=-2$) for localized spins. The α value shows a complicated density dependence which is accompanied by a density variation of a heat capacity isotherm at an extremely low temperature ($\approx 0.2\text{ mK}$). This anomaly is similar to the previously observed high-temperature behavior ($\alpha\approx-1$) of the lowest density solid in the second layer. Although quantitative explanations are lacking for these anomalies, they are likely due to the high frustration caused by competing ferromagnetic and antiferromagnetic multiple-spin exchange interactions at least up to the six-spin exchange. We find that the excess heat-capacity (C_{ex}) due to the amorphous ^3He adsorbed on substrate heterogeneities is certainly not an origin of the anomalous behavior in C of the uniform submonolayer. Only at and below the density for the $\sqrt{3}\times\sqrt{3}$ commensurate phase ($\rho=6.4\text{ nm}^{-2}$) heat capacity bumps at around 20 mK are observed. We suggest the possibility of spin-polaron effects caused by delocalized vacancies to explain this anomaly.

DOI: 10.1103/PhysRevB.65.104524

PACS number(s): 67.70.+n, 67.80.-s, 75.70.Ak

I. INTRODUCTION

First- and second-layer solid ^3He physisorbed on a graphite surface are ideal two-dimensional (2D) quantum spin systems with a nuclear spin of $S=1/2$.¹ The magnetic properties of the second-layer ^3He are known to vary from antiferromagnetic (AFM) to ferromagnetic (FM) ones with increasing areal density (ρ). Recently it has become accepted that competition among several multiple-spin exchange (MSE) interactions up to the six-spin exchange plays an important role in the density dependence of the magnetism.²⁻⁴

In previous nuclear-spin heat-capacity (C) measurement for the second-layer ^3He by Ishida *et al.*,⁵ the double-peak feature was observed in the AFM $\sqrt{7}\times\sqrt{7}$ solid phase, which is commensurate against the first-layer ^3He , while the simple 2D Heisenberg behavior was seen in the higher density FM solids. The double-peak structure indicates the existence of many low-lying states, and possibly the quantum spin-liquid ground state.⁵ They also observed a curious temperature dependence $C\propto T^{-1}$ as well as a small bump at high temperatures instead of the expected $C\propto T^{-2}$ behavior for any localized spin systems. The microscopic origin of these high-temperature anomalies was not known until now. On the other hand, the normal T^{-2} behavior was observed in the FM region.

Greywall and Busch (GB)⁶ were the first to measure nuclear-spin heat capacities in the submonolayer solid on graphite in a temperature range between 2 and 20 mK. They claimed that the temperature dependence of C in the lowest density $\sqrt{3}\times\sqrt{3}$ solid is closer to T^{-1} rather than T^{-2} . More recently, we reported the same anomaly ($C\propto T^{-1}$) in the

submonolayer solid at a few selected densities, but in a much wider temperature range ($0.1\text{ mK}\leq T\leq 20\text{ mK}$).⁷ Studies of the submonolayer have several advantages over the studies of the second layer. For example, the absence of fluid overlayers, which have large heat capacities at high temperatures, in an interesting density region makes an analysis of experimental results much simpler. This absence is due to the fact that the promotion to the second layer takes place only after the first layer is highly compressed. Instead, there are technical difficulties in experimental studies of the submonolayer, since the nuclear-spin exchange interactions are much smaller than those in the second layer.

In this paper we present a more comprehensive study of the anomaly of C in the submonolayer ^3He on graphite. They show that a $C\propto T^\alpha$ ($\alpha\approx-1$) behavior indeed holds over an anomalously wide temperature range, and exists in almost the whole density region for the submonolayer solid with some extra structures at several densities. This is in clear contrast to what was observed in the second-layer solid.^{5,8} The results strongly suggest that the submonolayer ^3He on graphite is a highly frustrated 2D magnetic system due to strong competition among MSE's. It is probably more frustrated than the second layer, and the observed anomalous behavior in the heat capacity creates challenges for theoretical investigations of this system.

II. EXPERIMENTAL TECHNIQUES

The apparatus and experimental techniques used in this work are basically the same as those in a previous work.⁵ The total surface area ($=390\text{ m}^2$) of Grafoil⁹ substrate was determined as follows. First we compared an adsorption iso-

therm of ^3He at 4.2 K with the data of Morhard *et al.*¹⁰ and Goellner *et al.*¹¹ The accuracy of this comparison is within several percent. Then we fine tuned by comparing measured heat-capacity isotherms, particularly peaks near 7.6 nm^{-2} at various fixed temperatures above 2.5 mK with those of GB. Due to different preparations of the substrate, the ratio of the heterogeneous surface to the homogeneous one is larger by a factor of 2 compared to our previous substrate ($\approx 14\%$).⁵

The ^3He films were carefully prepared in order to avoid a possible density inhomogeneity or crystalline imperfections. Films with desired densities were made by introducing known amounts of ^3He gas into a calorimeter typically at 4.2 K or at about 10 K, and were annealed for 12 h at about 15 K, where the vapor pressure is sufficiently high to ensure the uniformity of the film density. The pressure was monitored with a strain capacitive gauge located close to the calorimeter. After the annealing the films were cooled slowly below 6 K, taking almost one day.

The heat capacity of the uniform film is obtained from the measured total heat capacity by subtracting the addendum and the excess heat capacity. The latter one (C_{ex}) is believed to arise from nuclear-spin degrees of freedom in the amorphous ^3He adsorbed on substrate heterogeneities such as boundaries of graphite platelets.⁵ As reported briefly elsewhere,¹² we have determined variations of C_{ex} with T and ρ for our Grafoil substrate in a wide density range (Fig. 1). The data points in the figure fall into two categories (the solid lines). This indicates that the amorphous ^3He also has a layering structure like that of the uniform film, i.e., the two lines correspond to the submonolayer and the sum of the submonolayer and second-layer amorphous ^3He . The layer promotion takes place at a certain density between $\rho=8.9$ and 9.5 nm^{-2} . In the following, we assume the density independence of the $C_{ex}(T)$, shown by the solid line labeled as ‘1st layer amorphous’ in Fig. 1, between 4.1 and 8.9 nm^{-2} ,

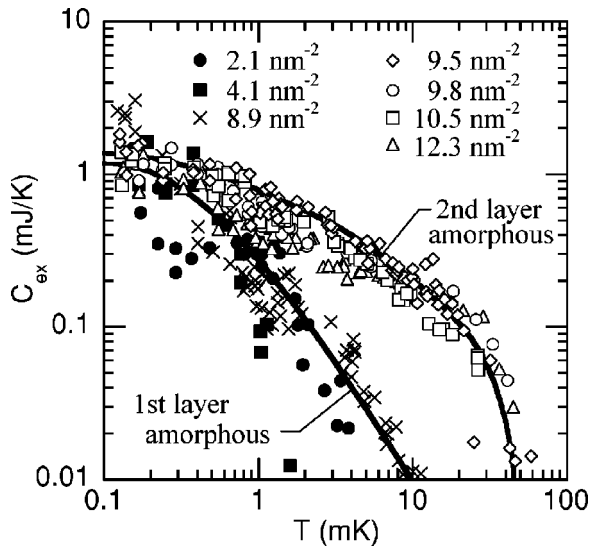


FIG. 1. Excess heat capacities (C_{ex}) which are attributed to the amorphous ^3He trapped on heterogeneities of Grafoil substrate (the surface area is 390 m^2). The data can be classified into two categories denoted by the solid lines, suggesting a layering structure. The layer promotion takes place between $\rho=8.9$ and 9.5 nm^{-2} .

which seems to be reasonable judging from the figure. More details of the experimental techniques to measure tiny heat capacities of a few millimole of ^3He down to $100 \mu\text{K}$ will be described elsewhere.¹³

III. EXPERIMENTAL RESULTS

Temperature variations of the measured heat capacities (C) of submonolayer solid ^3He at five selected densities, $\rho = 6.1, 6.4, 7.6, 8.2$ and 8.5 nm^{-2} out of 14 densities, are shown in Figs. 2(a) and 2(b).¹⁴ In Fig. 2(a) the data for $\rho \leq 7.6 \text{ nm}^{-2}$ are plotted, and in Fig. 2(b) we show those for $\rho \geq 7.6 \text{ nm}^{-2}$. At most of the densities anomalous T dependencies of C , $\propto T^\alpha$ ($-1.6 \leq \alpha \leq -0.7$) are seen. The data do not approach $C \propto T^{-2}$ behavior even in the high-temperature limit. Note that for any localized spin system α should approach -2 . Moreover, the data at 7.6 nm^{-2} seem to follow a simple power law with $\alpha = -1.2 \pm 0.1$, in a surprisingly wide temperature range more than two orders of magnitude ($0.2 \text{ mK} \leq T \leq 30 \text{ mK}$). Similar high-temperature anomalies were reported previously by GB in limited temperature and density regions.⁶ The present data show unambiguously that this behavior holds in much wider temperature and density regions. Only at 8.5 nm^{-2} and below about 1 mK is the normal exponent observed. Although one might suspect that this anomalous behavior might be a result of an inappropriate subtraction of C_{ex} , we cannot reproduce the normal T^{-2} behavior with any C_{ex} allowed within the experimental errors.

As shown in Fig. 3, heat-capacity isotherms at $T=5$ and 2.5 mK agree fairly well with GB's data within combined uncertainties in the two measurements. The isotherm at 0.2 mK has a sharp peak at $\rho=7.6 \text{ nm}^{-2}$, indicating a maximum effective exchange-frequency there. Note that only the vertical axis for the 0.2-mK isotherm is divided by a factor of 5. The same isotherm is also shown in Fig. 4(a) in the original scale. Although the peak itself was previously noted at the higher-temperature measurement,⁶ the present peak is much more pronounced because of combined effects between the much lower temperature and the smaller α value at this density. There is another, less pronounced, peak at 8.5 nm^{-2} which is also enhanced due to the smallness of the α value (≈ -2). The isotherm at 0.2 mK shows a steep drop just above 6.4 nm^{-2} , the stoichiometry density for the $\sqrt{3} \times \sqrt{3}$ registered phase [the R_{1a} phase in Fig. 4(d)]. The last two features could be difficult to recognize in the higher-temperature isotherms.

Figure 4(b) shows a density variation of the exponent α , determined in the following way. The data at lower temperatures where the C value is larger than 0.05 mJ/K were fitted to the simple power-law formula $C \propto T^\alpha$. Only for 6.1 and 6.4 nm^{-2} were the fittings performed for $C \geq 0.3 \text{ mJ/K}$ to avoid bumps near 20 mK, which we will discuss in detail in Sec. IV C. The α value first increases as the density increases until 6.5 nm^{-2} . Above 7.5 nm^{-2} it decreases generally with density, but shows steep drops near 7.6 and 8.5 nm^{-2} . These structures take place consistently with the structures seen in the heat capacity isotherm [Fig. 4(a)].

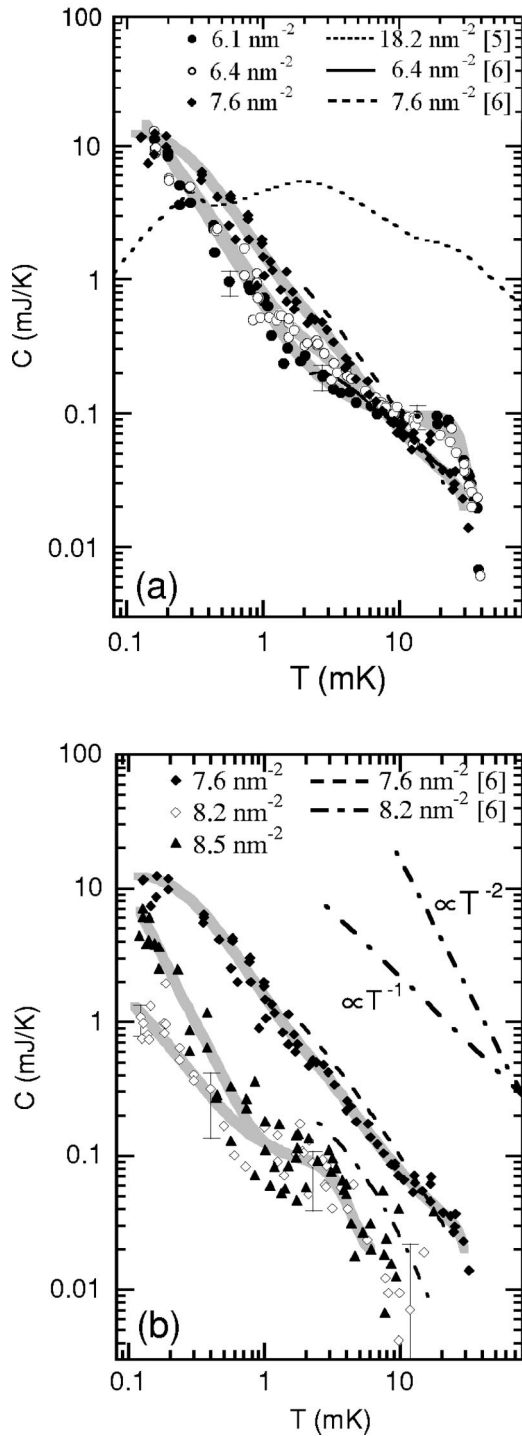


FIG. 2. Nuclear-spin heat capacities (C) of ^3He submonolayer solids adsorbed on graphite at 6.1 , 6.4 , and 7.6 nm^{-2} (1a) and 7.6 , 8.2 , and 8.5 nm^{-2} (1b). The contribution from amorphous ^3He adsorbed on substrate heterogeneities was already subtracted from these data (see text). For most of the densities, the temperature dependencies of C are anomalously weak compared to the normal $C \propto T^{-2}$ behavior. The solid (6.4 nm^{-2}), dashed (7.6 nm^{-2}), and dash-dotted lines (8.2 nm^{-2}) are from Ref. 6. The dotted line represents the data for the $\sqrt{7} \times \sqrt{7}$ commensurate solid in the second layer from Ref. 5.

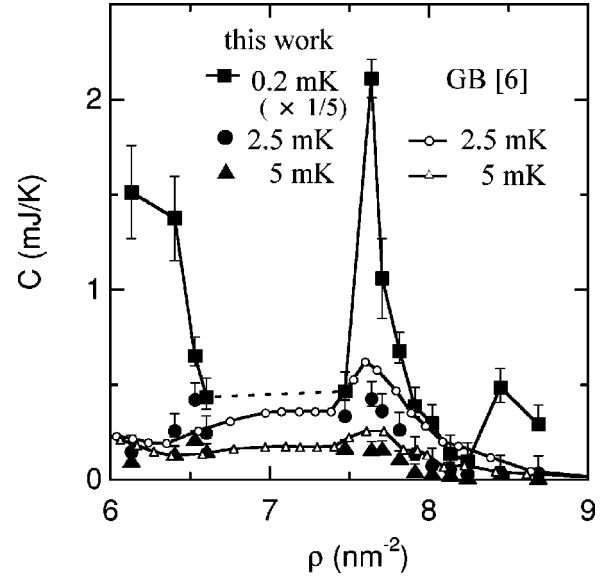


FIG. 3. Our heat-capacity isotherms (closed symbols) of submonolayer solid ^3He on graphite at 0.2 , 2.5 , and 5 mK are compared with GB's data (open symbols, Ref. 6). Note that the C values of 0.2 mK are divided by a factor of 5.

However, it should be noted that α is always larger than the normal value -2 in the whole density region for the solid phase except around $\rho = 8.5 \text{ nm}^{-2}$. These structures in the ρ dependence of α may look somewhat arbitrary, because the data scatterings are relatively large. However, the error bars shown in Fig. 4(b) are mainly due to uncertainties in the determination of C_{ex} . Thus, as long as the assumption that C_{ex} is ρ independent in this density range is correct, these fine structures should be real.

It is suggestive to compare the present results with what is known in the second-layer solid ^3He . The C data of Ishida *et al.*⁵ for the second-layer density (ρ_2)¹⁵ of 6.8 nm^{-2} are shown in Fig. 2 by a dotted line. A similarly anomalous $C \propto T^\alpha$ ($\alpha \approx -1$) behavior is seen in this low-density AFM $\sqrt{7} \times \sqrt{7}$ commensurate solid. In this case the characteristic temperature scale is higher by a factor of more than 10. This is due to the fact that magnitudes of the exchange interactions are different between the two layers approximately by that factor. In the submonolayer, owing to the much stronger adsorption potential from the substrate, tunneling paths for exchanging atoms are restricted more strictly to 2D space; thus the exchange frequencies are much lower. The α values determined from the existing second-layer data^{5,8} are plotted as a function of ρ_2 in Fig. 5(a). They are deduced from the data for $C \geq 0.1 \text{ mJ/K}$ at high densities and for $C \geq 2 \text{ mJ/K}$ for densities near the $\sqrt{7} \times \sqrt{7}$ phase to avoid the high-temperature bump in the case when the surface area is 450 m^2 . The α value decreases monotonically with increasing ρ_2 above 7.3 nm^{-2} , and then reaches the normal value ($= -2$) around 8.0 nm^{-2} . This density variation is different from that for the submonolayer solids observed in this work in several aspects. We will discuss these intriguing differences in Sec. IV in light of the MSE hypothesis.

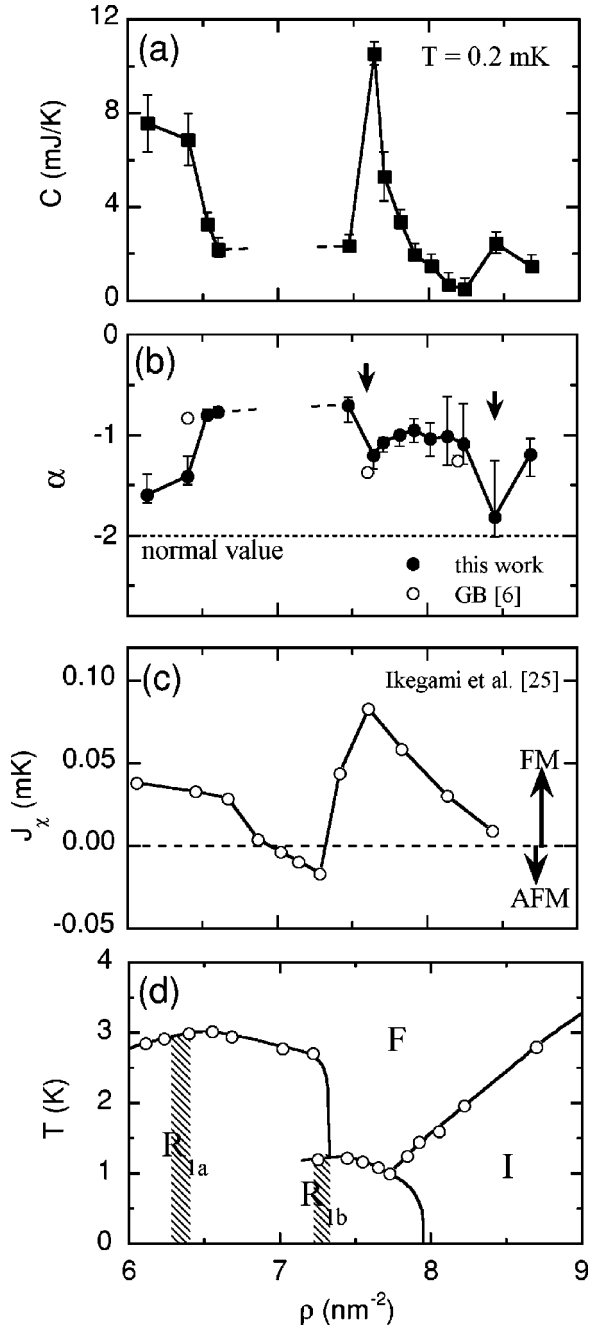


FIG. 4. (a) Heat-capacity isotherms of the submonolayer solid ${}^3\text{He}$ on graphite at $T=0.2$ mK. (b) The exponent α determined by fitting the data to $C \propto T^\alpha$ is plotted as a function of areal density. This work (closed circles); data from Ref. 6 (open circles). The horizontal dotted line is the normal α value ($= -2$) for any localized spins at high temperatures ($T \gg J_p$). The arrows indicate positions where the density dependence of α has dips presumably due to the formation of particular commensurate phases or some structural phase transitions (see text). (c) J_χ determined from the magnetization measurement (Ref. 25). (d) The structural phase diagram proposed by heat-capacity measurements (Refs. 6 and 32). R_{1a} , $\sqrt{3} \times \sqrt{3}$ commensurate phase; R_{1b} , hypothetical 2/5 commensurate phase proposed in Ref. 8; I , incommensurate phase; F , fluid phase. The errors shown in (a) and (b) are mainly due to those in the determination of C_{ex} and the addendum heat capacity.

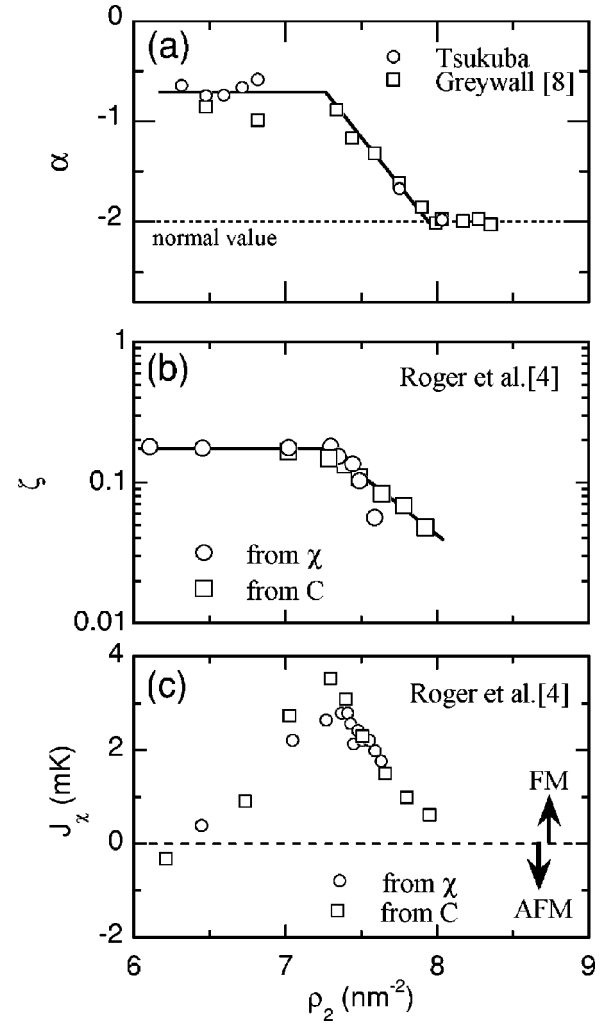


FIG. 5. (a) The exponent α determined from the high-temperature heat capacities in the second-layer solid ${}^3\text{He}$ plotted as a function of the second-layer density. The data from Ref. 5 and unpublished data by the Tsukuba group (open circles); from Ref. 8 (open squares). The line is a guide to the eye. (b) The frustration parameter ζ [see Eq. (1)] in the second layer from the heat-capacity (open circles) and magnetization data (open squares) after Ref. 4. The line is a guide to the eye. (c) J_χ determined from the heat capacity and magnetization measurements (Ref. 4).

IV. DISCUSSION

A. Frustration caused by competing MSE's

The frustration due to competing AFM and FM MSE's is one of the most plausible explanations for the anomalous T dependencies of C in submonolayer solids. In 3D bcc ${}^3\text{He}$ at 22.69 cm 3 /mol, the Néel temperature ($T_N=0.28$ mK) at zero field for an AFM ordered phase (u2d2 phase 16) is suppressed by a factor of 3 from the highest transition temperature ($=0.96$ mK) for another AFM ordered phase in magnetic fields. 17 This suppression of long-range ordering is attributed to the frustration caused by the MSE competition. It is also known that, with decreasing temperature above T_N , the specific heat deviates negatively from the leading T^{-2} term in the high-temperature series expansions (HTSE) for C by a large amount. 18 This is explained by the MSE competi-

tion suppressing the short-range ordering in the paramagnetic phase. Note that the deviation is small and positive in the Heisenberg model without frustration. These frustration effects should be more important in lower dimensions in general. That is why the disordered ground state is expected in the 2D AFM phase of the second layer ^3He on graphite, where the MSE competition is believed to be essential (spin liquid hypothesis).^{5,19}

Within the MSE model the gradual decrease of α with increasing density in the second layer is explained as a gradual suppression of frustration. This is demonstrated well by plotting the logarithm of the *frustration parameter* ζ ,

$$\zeta = -(J_4 - 2J_5)/(J_2 - 2J_3), \quad (1)$$

introduced by Roger *et al.*⁴ as a function of ρ_2 [Fig. 5(b)], and comparing it with Fig. 5(a). Here J_2, J_3, J_4 and J_5 are two-, three-, four-, and five-spin exchange frequencies, respectively, appearing in the MSE Hamiltonian:

$$H = (J_2 - 2J_3) \sum P_2 + J_4 \sum (P_4 + P_4^{-1}) - J_5 \sum (P_5 + P_5^{-1}) + J_6 \sum (P_6 + P_6^{-1}). \quad (2)$$

In this expression, P_n and P_n^{-1} are cyclic permutation operators for n spins and their inverse permutation operators, respectively. These exchange frequencies were determined by Roger *et al.*⁴ by fitting existing heat capacity and magnetization data to the HTSE formulas based on the MSE Hamiltonian. The denominator and numerator in Eq. (1) represent the effective two-spin and effective four-spin exchange frequencies, respectively. Clearly, $\ln \zeta$ and α have similar ρ_2 dependencies each other looking at Figs. 5(a) and 5(b). It is also shown in the HTSE calculation²⁰ that the specific heat at a fixed scaled temperature T/J_C decreases dramatically with increasing J_4 , i.e., increasing ζ , which is equivalent to an effective increase of α . Here J_C is a coefficient of the leading term in the HTSE for C as follows:

$$C = Nk_B(9/4)J_C^2/T^2 + O(T^{-3}). \quad (3)$$

Therefore, the anomalously large α (≈ -1) seems to be a direct consequence of the large- ζ value, which is measure of the higher order MSE's. If so, this scenario should also be applicable to the submonolayer.

It is not possible, however, to determine ζ values for the submonolayer solids because of the fact that the anomalous behavior ($C \propto T^\alpha, \alpha > -2$) holds in such a wide temperature range, e.g., $0.1 \text{ mK} \leq T \leq 20 \text{ mK}$ for $\rho = 7.6 \text{ nm}^{-2}$. Nevertheless, there is circumstantial evidence that the higher-order exchanges are indeed important, and that the frustration is even stronger in the submonolayer than in the second layer. For example, a preliminary path-integral Monte Carlo calculation²¹ actually suggests large ζ values. It is also expected that J_2 becomes less important as the exchange paths are spatially restricted. This is a general tendency of atomic exchanges with hard cores, which was shown experimentally in bcc ^3He .²² The exchange paths in the first layer are restricted more strictly in 2D by the stronger adsorption poten-

tial ($\approx -190 \text{ K}$) (Ref. 23) than in the second layer ($\approx -40 \text{ K}$), and laterally as well by the stronger potential corrugation. Therefore, if we accept the correlation between α and ζ , the large α values obtained in this work can be explained at least qualitatively by high frustration caused by the competing MSE's.

We speculate that at the two particular densities near 7.6 and 8.5 nm^{-2} , the submonolayer has some sort of commensurability to the underlying graphite basal plane or some structural phase transitions.²⁴ If so, such structures may favor particular exchange processes, perhaps three-spin exchange, and hence reduce the frustration, resulting in dips in the α vs ρ plot. In previous experiments,^{8,25} however, no similar features were observed at the corresponding densities. Such fine structures might be ignored in those measurements if the anomalies locate on very narrow density windows, as is expected for commensurate phases or if the measured temperature range is not low enough.

We now turn to the observed decrease of α below 6.5 nm^{-2} , where the solid is in the $\sqrt{3} \times \sqrt{3}$ commensurate phase. Recently Ikegami *et al.*²⁵ showed that J_χ ($\equiv \theta/3$, where θ is the Weiss constant) is positive (ferromagnetic) in this region. They argued the possible predominance of J_3 over J_2 based on a geometrical consideration of the potential corrugation in that registered phase. This argument was supported by a recent WKB calculation of the MSE's,²⁶ and is consistent with the smaller α values, which means lower frustration, obtained below 6.4 nm^{-2} in this work. Another possibility is that vacancies, which may exist in the commensurate solid below 6.5 nm^{-2} , promote lower-order exchanges such as J_2 or J_3 and suppress the frustration. On the other hand, α seems to be largest in the intermediate density region between the commensurate and incommensurate phases ($6.5 \text{ nm}^{-2} \leq \rho \leq 7.5 \text{ nm}^{-2}$), although we did not survey the central part of this region. Interesting domain-wall structures or commensurate phases are predicted to exist in this region for a ^4He submonolayer.^{27,28} It is likely that the MSE competition near the heavy domain walls is different from that in the uniform domains.

B. Other possibilities

In this subsection, we will discuss possible explanations for the anomalous α values other than the MSE competition. One possibility is that our assumption that the series of higher-order exchanges in the MSE Hamiltonian can be truncated at the sixth order is irrelevant. If we cannot ignore contributions from much higher-order exchanges such as 12 or 18 spin exchanges regardless of an opposing prediction by the WKB calculation,²⁹ J_C could be much larger in magnitude than J_χ . If so, the temperature range of our measurement is not high enough to observe the limiting T^{-2} behavior. Note that the magnitude of J_χ can be suppressed significantly due to cancellation among FM and AFM MSE's, but J_C cannot.

Let us now consider another scenario to try to reproduce the measured T dependence of C as a sum of the HTSE formula and contributions associated with some other degrees of freedom. One candidate for those is the spin polaron

effect induced by the vacancies activated thermally or spontaneously. However, so far there have been no quantitative calculations of heat-capacity contributions (C_{pl}) from polarons for the triangular (*nonbipartite*) lattice nor for any lattices with the multiple-atom exchanges. Instead, for the case of an $S=1/2$ fermion system on a square (*bipartite*) lattice, approximate $C_{pl} \propto T^{-1/2}$ behavior at low temperatures is predicted,³⁰ and C_{pl} may have rounded double peaks at temperatures near $T \approx 0.1t$ and t .³¹ Here t is the hopping frequency of a vacancy which should be one or two orders of magnitude larger than J . It is, however, rather difficult to imagine that fairly large amounts of vacancies survive in the high-density incommensurate solids. In this regime, rather than the vacancies, interstitial atoms or the domain walls would play some important roles in the extra heat capacities.

Another possibility is the finite-temperature effect on quantum tunneling in atom exchanges. In principle, with increasing temperature the exchange frequency should increase due to thermally assisted tunneling between excited levels. This may explain the positive deviation of C from the normal T^{-2} behavior at high temperatures. According to Roger's WKB calculation,²⁹ the MSE frequency (J_p) is given by

$$J_p \propto \exp(-\sqrt{V_p} L_p), \quad (4)$$

where L_p is the exchange path length in $2N$ -dimensional space, and V_p is the potential barrier height due to the hardcore repulsion among N atoms involved in the exchange process. L_p is longer and V_p is lower for higher-order MSE's. However, the finite-temperature effect should be negligible below 100 mK, at least for lower-order exchanges than J_6 . This is because V_p is estimated as of the order of several K,²⁹ and the energy separation between the ground and excited states should be of the same order. Roger argued that V_p would saturate as L_p increases for much higher-order exchanges such as a 32-spin ring exchange. This means that the thermal effect on those exchanges would be negligible as well. Moreover, if this effect is relevant, a deviation from the normal $C \propto T^{-2}$ behavior should develop exponentially as the temperature rises, which is not the experimental case.

The strong spin-lattice coupling may induce a similar finite-temperature effect on J_p . However, the Debye temperatures of the submonolayer solids are higher than 10 K.³² In addition, the more rapid approach of α to -2 at high densities in the second layer than in the first layer, in spite of the lower Debye temperature, seems to be contradictory to this assumption. Thus this mechanism should also be irrelevant.

In almost all previous heat-capacity measurements of ^3He thin films adsorbed on Grafoil, roughly T -independent excess heat capacities (C_{ex}) were observed at temperatures below several tens of mK, in addition to heat capacities of uniform 2D fluids or solids.^{5,8,33-35} From a comparison with heat-capacity data of ^3He films adsorbed on thoroughly heterogeneous substrates such as Vycor glass³⁶ or sintered silver powders,³⁷ C_{ex} is believed to arise from nuclear-spin degrees of freedom in the amorphous ^3He adsorbed on substrate heterogeneities such as boundaries of graphite platelets.⁵ As described in Sec. II, we have determined variations of C_{ex} with

T and ρ for our Grafoil substrate, and that $C_{ex}(T)$ for the submonolayer were already subtracted from our data plotted in Figs. 2–4. This means that the $C_{ex}(T)$ is not the origin of the anomalous α values. The knowledge of this T dependence of C_{ex} is essential to determine the exact T dependence of the spin heat capacity in the uniform submonolayer solid. This was not necessarily satisfied in the previous measurements.^{6,7} However, the situation is not so serious for second-layer solids, due to the large C values in the uniform solids. Eventually, the result does not change appreciably even though we reanalyze the data of Ref. 5 using the present T -dependent second-layer C_{ex} shown in Fig. 1.

C. Heat-capacity bumps at high temperatures

Finally we discuss the bump structure observed around 20 mK at $\rho=6.1$ and 6.4 nm^{-2} (see Fig. 2). A similar structure has been observed in the $\sqrt{7} \times \sqrt{7}$ commensurate solid in the second layer at almost the same temperature (≈ 30 mK).⁵ In this case, the possibility of remnant fluid contribution has been excluded, because the anomaly cannot be fitted by adding any fractions of the highest density fluid heat capacity to the solid heat capacity without the bump. The same is true for the $\sqrt{3} \times \sqrt{3}$ phase in the submonolayer in this work.

These bumps are likely due to the spin polaron effects induced by the vacancies which were briefly discussed in Sec. IV B. As described there, the heat-capacity contributions from the polarons C_{pl} for the $S=1/2$ fermion system on a square lattice are predicted to be the rounded double peak, and to have the asymptotic $T^{-1/2}$ behavior below the peak temperatures.^{30,31} If we assume $t \approx 200$ mK for the hopping frequency of the vacancy, this model may somehow reproduce the observed overall temperature dependencies at 6.1 and 6.4 nm^{-2} by adding C_{pl} to the normal T^α ($\alpha \approx -2$) dependence of the exchange part. However, it should be noted that the registered phases in both the first and second layers have triangular lattices rather than the square lattices to which the theories are directly applicable. Moreover, the theories do not take into account next-nearest-neighbor hopping or multiple-atom exchanges. Nevertheless, the fact that bumps are observed only in the lowest density commensurate solids, and disappear in the incommensurate solids, is still encouraging for this hypothesis. Further experimental and theoretical studies are clearly necessary to solve this problem. Similar bump structures may be seen near 8.2 and 8.5 nm^{-2} as well, but these are within the experimental errors mainly due to the ambiguity in C_{ex} , and would not be true unlike the bumps near the $\sqrt{3} \times \sqrt{3}$ phase.

V. CONCLUSIONS

To summarize, we have measured heat capacities (C) of the submonolayer solid ^3He adsorbed on graphite down to $100 \mu\text{K}$. Anomalous temperature dependencies, $C \propto T^\alpha$ ($-1.6 \leq \alpha \leq -0.7$), have been observed over two orders of magnitude in temperature in a wide areal density range ($6.1 \text{ nm}^{-2} \leq \rho \leq 8.7 \text{ nm}^{-2}$). The exponent α has a complicated density dependence, but is always less negative than the expected value ($= -2$) for localized spins at high tem-

peratures, except at a particular density ($= 8.5 \text{ nm}^{-2}$). Comparing with the previously known behavior in a second-layer solid, we attribute this anomaly to the high frustration caused by competing ferromagnetic and antiferromagnetic multiple-spin exchange interactions up to the six-spin exchange. However, there are currently no quantitative explanations for the unexpected behavior. Careful measurements of the excess heat capacity (C_{ex}) due to the amorphous ^3He trapped on substrate heterogeneities allowed us to exclude a possible influence of C_{ex} on the anomalous α values. Finally, we discussed the possibility of spin-polaron effects caused by vacancies to explain the observed high-temperature bump anomaly in the heat capacity for the $\sqrt{3} \times \sqrt{3}$ commensurate phase.

This work demonstrated that the submonolayer solid ^3He is an interesting two-dimensional quantum spin system with

the multiple-spin exchanges. There remain many still unsolved and fundamentally interesting questions in this system. Hopefully we have stimulated further experimental and theoretical studies to solve them.

ACKNOWLEDGMENTS

The authors are thankful to H. Godfrin, K. Kubo, T. Takagi, D. S. Hirashima, and M. Ogata for their stimulating discussions. We also acknowledge technical assistance by M. Furuya, Y. Mori, and K. Yokoyama. This work was supported by Grants-in-Aid for Scientific Research from the Ministry of Education, Culture, Sports, Science and Technology, Japan, the NEDO International Joint Research Grant, and the Cryogenics Center of the University of Tsukuba.

-
- ¹H. Godfrin and H. J. Lauter, in *Progress in Low Temperature Physics*, edited by W. P. Halperin (Elsevier, Amsterdam, 1995), Vol. XIV, p. 213, and references therein.
- ²M. Roger, *Phys. Rev. Lett.* **64**, 297 (1990).
- ³M. Siqueira, J. Nyéki, B. Cowan, and J. Saundears, *Czech. J. Phys.* **46**, Suppl. S6, 3033 (1996).
- ⁴M. Roger, C. Bäuerle, Yu.M. Bunkov, A.-S. Chen, and H. Godfrin, *Phys. Rev. Lett.* **80**, 1308 (1998); M. Roger, C. Bäuerle, and H. Godfrin, *J. Low Temp. Phys.* **113**, 249 (1998).
- ⁵K. Ishida, M. Morishita, K. Yawata, and Hiroshi Fukuyama, *Phys. Rev. Lett.* **79**, 3451 (1997).
- ⁶D.S. Greywall and P.A. Busch, *Phys. Rev. Lett.* **65**, 2788 (1990).
- ⁷M. Morishita, H. Nagatani, and Hiroshi Fukuyama, *J. Low Temp. Phys.* **113**, 271 (1998).
- ⁸D.S. Greywall, *Phys. Rev. B* **41**, 1842 (1990); D.S. Greywall and P.A. Busch, *Phys. Rev. Lett.* **62**, 1868 (1989).
- ⁹Grafoil (grade GTA) is an exfoliated graphite sheet manufactured by Union Carbide Corporation.
- ¹⁰K.-D. Morhard, J. Bossy, and H. Godfrin, *Phys. Rev. B* **51**, 446 (1995).
- ¹¹G.J. Goellner, J.G. Daunt, and E. Lerner, *J. Low Temp. Phys.* **21**, 347 (1975).
- ¹²M. Morishita, H. Nagatani, and Hiroshi Fukuyama, *Physica B* **284-288**, 228 (2000). Note that the Grafoil substrate used in this work is not the same as that used in Ref. 5, and C_{ex} for this work is almost twice that in the previous one.
- ¹³Hiroshi Fukuyama, M. Morishita, and K. Ishida (unpublished).
- ¹⁴The preliminary results of this experiment were reported in M. Morishita, H. Nagatani, and Hiroshi Fukuyama, *Physica B* **284-288**, 220 (2000).
- ¹⁵In this paper, we estimated ρ_2 values from given ρ ones using the ρ_2 vs ρ relation proposed by M. Roger, C. Bäuerle, H. Godfrin, L. Pricoupenko, and J. Treiner, *J. Low Temp. Phys.* **112**, 451 (1998). Since it is based on the "Grenoble density scale," which gives about a 4% larger density than the "GB's scale" employed here (see Ref. 10), we have corrected the ρ_2 vs ρ relation of Roger *et al.* taking account of this discrepancy. The correction does not change density dependencies of magnetic properties of the second-layer solid qualitatively nor conclusions of this paper.
- ¹⁶D.D. Osheroff, M.C. Cross, and D.S. Fisher, *Phys. Rev. Lett.* **44**, 792 (1980).
- ¹⁷Hiroshi Fukuyama, T. Fukuda, T. Okamoto, H. Akimoto, H. Ishimoto, and S. Ogawa, *Physica B* **169**, 197 (1991), and references therein.
- ¹⁸H. Fukuyama, Y. Miwa, A. Sawada, and Y. Masuda, *J. Phys. Soc. Jpn.* **53**, 916 (1984).
- ¹⁹Hiroshi Fukuyama and M. Morishita, *Physica B* **280**, 104 (2000).
- ²⁰M. Roger, *Phys. Rev. B* **56**, R2928 (1997).
- ²¹B. Bernu (private communication).
- ²²Hiroshi Fukuyama, T. Okamoto, T. Fukuda, H. Akimoto, H. Ishimoto, and S. Ogawa, *Phys. Rev. Lett.* **67**, 1274 (1991).
- ²³F. Joly, C. Lhuillier, and B. Brami, *Surf. Sci.* **264**, 419 (1992).
- ²⁴M. Morishita and T. Takagi, *Phys. Rev. Lett.* **87**, 185301 (2001).
- ²⁵H. Ikegami, K. Obara, D. Ito, and H. Ishimoto, *Phys. Rev. Lett.* **81**, 2478 (1998).
- ²⁶H. Ashizawa and D.S. Hirashima, *Phys. Rev. B* **62**, 9413 (2000).
- ²⁷T. Halpin-Healy and M. Kardar, *Phys. Rev. B* **34**, 318 (1986).
- ²⁸D.S. Greywall, *Phys. Rev. B* **47**, 309 (1993).
- ²⁹M. Roger, *Phys. Rev. B* **30**, 6432 (1984).
- ³⁰M. Héritier and P. Lederer, *Phys. Rev. Lett.* **42**, 1068 (1979).
- ³¹R. Raghavan and V. Elser, *Phys. Rev. Lett.* **75**, 4083 (1995).
- ³²S.V. Hering, S.W. Van Sciver, and O.E. Vilches, *J. Low Temp. Phys.* **25**, 793 (1976).
- ³³D.S. Greywall and P.A. Busch, *Phys. Rev. Lett.* **65**, 64 (1990).
- ³⁴M. Morishita, K. Ishida, K. Yawata, H. Nagatani, and Hiroshi Fukuyama, *J. Low Temp. Phys.* **110**, 351 (1998).
- ³⁵A. Casey, H. Patel, J. Nyéki, B.P. Cowan, and J. Saunders, *J. Low Temp. Phys.* **113**, 293 (1998).
- ³⁶A. Golov and F. Pobell, *Phys. Rev. B* **53**, 12 647 (1996).
- ³⁷D.S. Greywall and P.A. Busch, *Phys. Rev. Lett.* **60**, 1860 (1988).